

Connected in bad times and in good times: Empathy induces stable social closeness

Empathy and stable social closeness

Anne Saulin^{1*}, Chih-Chung Ting², Jan B. Engelmann^{3,4,5}, & Grit Hein¹

1 University Hospital Würzburg, Department of Psychiatry, Centre of Mental Health, Psychosomatic and Psychotherapy, Translational Social Neuroscience Unit, Würzburg, 97080, Germany

2 General Psychology, Universität Hamburg, Hamburg, 20246, Germany

3 Center for Research in Experimental Economics and Political Decision Making, University of Amsterdam, Amsterdam, 1001, the Netherlands

4 Amsterdam Brain and Cognition, University of Amsterdam, Amsterdam, 1001, the Netherlands

5 Behavioral and Experimental Economics, The Tinbergen Institute, Amsterdam, 1082, the Netherlands

*corresponding author:

Anne Saulin

saulin_a@ukw.de

keywords: empathy, social closeness, reinforcement learning, fMRI, STS, TPJ, IFG, AI

Abstract

Humans need social closeness to prosper. There is evidence that empathy can induce social closeness. However, it remains unclear how empathy-related social closeness is formed and how stable it is as time passes. We applied an acquisition-extinction paradigm combined with computational modelling and fMRI, to investigate the formation and stability of empathy-related social closeness. Participants observed painful stimulation of another person with high probability (acquisition) and low probability (extinction), and rated their closeness to that person. The results of two independent studies showed increased social closeness in the acquisition block that resisted extinction in the extinction block. Providing insights into underlying mechanisms, reinforcement learning modelling revealed that the formation of social closeness is based on a learning signal (prediction error) generated from observing another's pain, whereas maintaining social closeness is based on a learning signal generated from observing another's pain relief. The results of a control study indicate that this feedback recalibration is specific to learning of empathy-related social closeness. On the neural level, the recalibration of the feedback signal was associated with neural responses in anterior insula and adjacent inferior frontal gyrus and the bilateral superior temporal sulcus/temporo-parietal junction. Together, these findings show that empathy-related social closeness generated in bad times, i.e., empathy with the misfortune of another person, transfers to good times, and thus may form one important basis for stable social relationships.

Significance Statement

Humans feel close to others if they empathize with them. Here we test whether this feeling of social closeness remains if empathy is no longer elicited. Combining mathematical learning models and functional magnetic-resonance imaging, we find that empathy with others' pain establishes stable social closeness that is maintained even if the other person is feeling well again. Explaining the mechanism, we show that the stability of empathy-induced social closeness is based on the recalibration of an empathy-related learning signal in the anterior insula/inferior frontal gyrus and the temporo-parietal junction. These findings reveal how empathy maintains social closeness and thus contributes to the formation of stable social relationships.

Introduction

Feeling close to other people is a principal human need (Baumeister & Leary, 2017; Hill, 2009). Documenting its importance, social closeness is linked to an increase in happiness, well-being (Kok & Fredrickson, 2014) and mental health (Cowan, Pham, Elvevåg, & Cohen, 2021; Dempsey et al., 2021), and influences hormone levels associated with altruistic motivation (Brown et al., 2009). Moreover, feeling socially close enhances the willingness to behave prosocially towards others (de Waal, Leimgruber, & Greenberg, 2008; Passarelli & Buchanan, 2020; Spaans et al., 2018).

One process that has been linked to increased social closeness is increased empathy (Beeney, Franklin, Levy, & Adams, 2011; Morelli, Lieberman, & Zaki, 2015). Empathy enables us to share another's emotions, and thereby, provides an important way to connect with other people. As such, empathy has been characterized as the glue that holds relationships and societies together (Calloway-Thomas, Arasaratnam-Smith, & Deardorff, 2017; Witenberg & Thomae, 2016). However, so far, it is unclear how long empathy-related social closeness lasts and whether it persists in the absence of empathy-inducing experiences. One experience that has been shown to incite empathy is observing another person in pain or misfortune (Beeney et al., 2011; Marsh, 2018; Xu, Zuo, Wang, & Han, 2009). Based on influential models from social psychology (Davis, 1983; Hein, Qi, & Han, 2021), observing others in pain results in sharing the other's emotions (called affective empathy) and thoughts or intentions (called cognitive empathy or theory of mind). Moreover, it has been shown that empathic responses (Hein, Engelmann, Vollberg, & Tobler, 2016) and empathy-related behaviors (Lockwood, Apps, Valton, Viding, & Roiser, 2016) can be shaped by learning.

Uncovering associated neural regions, previous studies have associated affective empathy with neural responses in the anterior cingulate cortex (ACC) and the anterior insula (AI), extending to the adjacent inferior frontal gyrus (IFG) (Cutler & Campbell-Meiklejohn, 2019; Dvash & Shamay-Tsoory, 2014; Fan, Duncan, de Greck, & Northoff, 2011; Preckel, Kanske, & Singer,

2018; Schurz et al., 2021; Stietz, Jauk, Krach, & Kanske, 2019; Walter, 2012). Supporting the close link between empathy and social closeness, neural activation in AI and IFG (Beeney et al., 2011) as well as ACC (Müller-Pinzler, Rademacher, Paulus, & Krach, 2015) were also found to change with varying degrees of social closeness. Cognitive empathy was mainly related to neural activation of the medial prefrontal cortex (mPFC), the superior temporal sulcus (STS), the temporal poles (TP), and the temporo-parietal junction (TPJ; Cutler & Campbell-Meiklejohn, 2019; Dvash & Shamay-Tsoory, 2014; Preckel et al., 2018; Schurz et al., 2021; Stietz et al., 2019).

Taken together, these previous studies showed that observing the suffering of another person (e.g., pain) activates neural circuits that have been associated with affective and cognitive empathy. Furthermore, there is evidence that these networks can be modulated by basic learning processes and that changes in empathy-related neural processes is linked to social behaviour and social closeness (Hein, Engelmann, et al., 2016; Krienen, Tu, & Buckner, 2010; Lockwood et al., 2016; Stevens & Taber, 2021; Weisz & Zaki, 2018). However, it is unknown whether empathy-related closeness still persists if empathy is no longer activated. In other words, does empathy-related social closeness prevail once the other person is feeling better and thus may no longer need empathy?

Here, we used an adapted acquisition-extinction paradigm (Dunsmoor et al., 2018; Palminteri, Khamassi, Joffily, & Coricelli, 2015; Shiban, Wittmann, Weißinger, & Mühlberger, 2015), reinforcement learning modelling, and functional magnetic resonance imaging (fMRI) to address this question in two independent studies. In an additional control study, we tested whether the observed results are specific for empathy-related closeness or reflect general learning-related changes in social closeness that also occur in other social contexts.

Participants inside the fMRI scanner (Study 1) and in the laboratory (Study 2) observed painful stimulation of another person known to elicit empathy for pain (Beeney et al., 2011; Grynberg & Konrath, 2020; Hein, Engelmann, et al., 2016; Lamm, Batson, & Decety, 2007; Marsh, 2018) in two conditions: a treatment condition and a control condition. In the first block

of the treatment condition (the acquisition block), participants observed painful stimulation of the other person with high probability (80%). In a second block (the extinction block), they observed the other receive painful stimulation with low probability (20%). In the control condition, participants observed painful stimulation in another person at chance level in both blocks (50%; **Figure 1A**). In each trial, after observing the stimulation of the other person, participants rated their emotional reaction to the stimulation, and subsequently indicated how close they felt to the other. To do so, they moved a mannequin (representing themselves) towards or away from a mannequin representing the other person (**Figure 1B**).

This set up allowed us to investigate the formation of empathy-related closeness in the acquisition block, and the stability of empathy-related closeness in the extinction block. To formalize the dynamic changes in social closeness with changing activation of empathy (i.e., after observing pain or non-pain in the other), we used a set of reinforcement learning models. Reinforcement-learning models mathematically describe the process of learning specific stimulus-outcome (i.e., reward vs. punishment) associations via trial and error (Rescorla & Wagner, 1972), which can be extended to associations between persons and outcomes. The Rescorla-Wagner model assumes that learning is driven by prediction errors, reflecting the difference between an observed and an expected feedback or outcome.

Inspired by previous work demonstrating that watching others receive painful stimulation elicits empathy (Beeney et al., 2011; Grynberg & Konrath, 2020; Hein, Engelmann, et al., 2016; Lamm et al., 2007; Marsh, 2018) and that empathy is linked to social closeness (Morelli et al., 2015), we hypothesized that watching another person receiving pain elicits a learning signal that is used to update social closeness. In more detail, we assume that empathy elicited by observing another person in pain increases social closeness that deviates from the prior expectation of felt social closeness. This empathy-related deviation of expected social closeness may generate a prediction error that in turn results in a dynamic update of social closeness depending on the “empathy reinforcer” (i.e., observing another’s in pain). In the acquisition block with frequent empathy reinforcers, participants should show a learning-related increase

in social closeness, captured by a dynamic increase in closeness ratings that reflects the respective prediction error estimate from our learning model. In the extinction block, when the other person only occasionally received empathy-inducing painful stimulation, we hypothesized a learning-related decay of empathy-related social closeness. However, if empathy-related closeness resists extinction, empathy-related social closeness should not decay when empathy reinforcers become rare in the extinction block, i.e., we should find no significant differences in closeness ratings between the acquisition and the extinction block. On a neural level, learning-related changes and the extent to which empathy-related social closeness resists extinction should be associated with changes in activation in brain regions related to cognitive empathy such as the TPJ, the STS, the mPFC and the temporal poles, and to regions related to affective empathy such as the AI and the adjacent IFG, and the anterior and mid ACC.

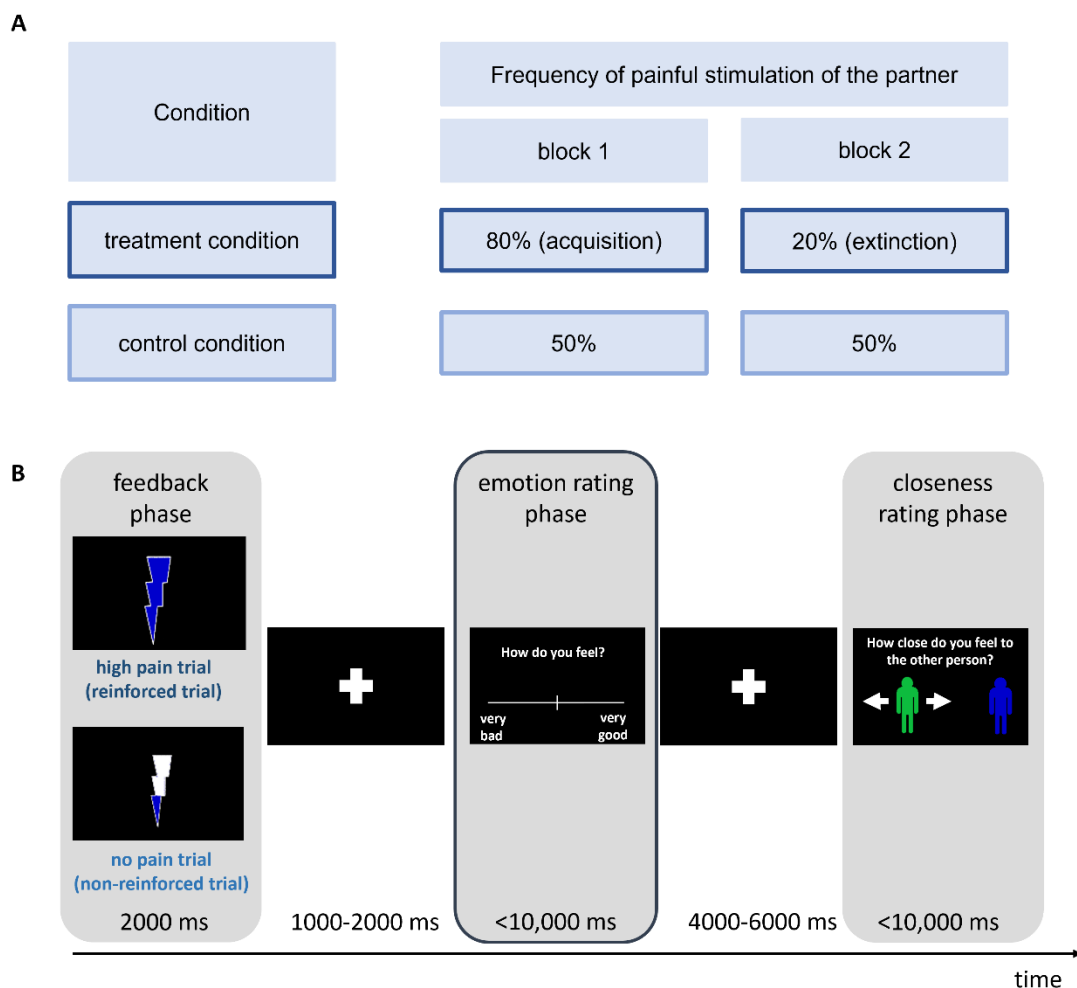


Figure 1. Visualization of the design and trial structure. (A) Participants sequentially underwent two counterbalanced conditions. In the treatment condition, they interacted with a first partner and performed two blocks of the motive task. In block 1, empathy was reinforced in 80% of the trials and in block 2 in 20% of the trials. They performed the same tasks again with a new interaction partner in the control condition. Here, empathy was reinforced in 50% of the trials in both blocks. The order of treatment and control conditions was counterbalanced across participants. (B) At the beginning of each trial participants observed that the other person received a painful stimulation (high pain trial = reinforced trial) or a non-painful stimulation (no-pain trial = non-reinforced trial). Then participants rated how they felt after observing this feedback. After 4000-6000 ms, participants (green mannequin) indicated how close they felt to the other person.

Materials and Methods

Participants

We recruited 107 right-handed healthy female participants via online platforms and flyers posted around the university campus in Würzburg (convenience sample, see **Table 4** for mean age and spread). Participants were assigned to three different studies: two studies investigating the formation and stability of empathy-related social closeness (one fMRI and one behavioural replication study), and one behavioural control study. We trained two female students that served as confederates in all three studies.

We chose female participants as well as female confederates to control for gender and avoid cross-gender effects. The confederates were students who had been trained to act as naïve participants. We ensured that participants did not know either of the confederates prior to the experiment by asking confederates beforehand. Before the experiment began, written informed consent was obtained from all the participants. The study was approved by the local ethics committee (268/18). Participants received monetary compensation (26.80 ± 3.30 Euros (mean \pm sd)). Monetary compensation was based on a fixed show-up fee and an individual pay-out based on the behavior in a decision task, which participants performed in addition.

We had to exclude seven data sets (five from the fMRI study and one each from the behavioral replication and the control study), because the estimation of learning models was not possible due to a lack of variance in ratings (four participants), falling asleep (two participants), or technical problems (one participant). Thus, we analyzed 46 data sets for the fMRI study, 27 data sets for the behavioral replication study and 27 data sets for the control studies. The mean age was comparable between studies ($F(2, 106) = 0.99, p = .376$, see **Table 4** for an overview of sample characteristics). A post-hoc sensitivity analysis using G*Power 3.1 indicated that given $\alpha = 5\%$, and considering 3 predictors in the regression model, the sample sizes of the respective studies had 80% power to detect a true effect with an effect size of $f \geq 0.18$ ($F = 2.68$)

in the fMRI study, and an effect size of $f \geq 0.23$ ($F = 2.73$) in the behavioral replication and the control studies.

fMRI study and behavioral replication study

Procedure

Prior to the tasks, the individual thresholds for pain stimulation (see section pain stimulation for details) were determined for the participants and the confederates. Thus, participants had a first-hand experience of the pain stimulation they would observe in others.

Next, the participants and confederates were assigned their different roles in a manipulated lottery of drawing matches. Participants always drew the last match in order to ensure she was assigned her designated role (observer). The confederates were assigned the role of pain recipients and served as treatment or control partner counterbalanced across participants. In the fMRI study, the respective confederate (treatment partner in the treatment condition and control partner in the control condition) was seated on a chair to the left of the participant with her hand visible to the participant. In the behavioral replication study, the respective confederate was seated next to the participant in a soundproof cabin facing the opposite direction such that no one could see the other's screen.

The fMRI experiment consisted of two conditions that were presented within-subject: (i) the treatment condition in which the participants observed painful stimulation of one of the confederates (treatment partner) with high probability (acquisition) and low probability (extinction), and (ii) the control condition in which participants observed painful stimulation of the other confederate (control partner) with chance probability in both blocks (**Figure 1**). In the acquisition block, participants observed that the partner received ostensibly painful stimulation in 80% of the trials, i.e., 80% empathy reinforcers. In the extinction block, they observed painful stimulation of the same confederate in 20% of the trials, i.e., 20% empathy reinforcers. In the control condition, participants observed painful stimulation of the second confederate in 50% of the trials of both blocks. Each block consisted of 25 trials. The order of treatment and control

conditions was counter-balanced across participants. Participants observed painful stimulation of different individuals in the treatment and the control condition to avoid spill-over effects and to keep the ostensible pain stimulation of the other person in a reasonable range.

Participants spent approximately 60 minutes in the scanner and the entire procedure took about 2.5 hours. The behavioural replication study lasted approximately 2 hours. To avoid possible reputation effects (Engelmann & Fischbacher, 2009; Gächter & Falk, 2002), which could influence participants' behavior, participants were informed at the beginning that they would not meet the others after the experiment. In more detail, at the end of the fMRI study, the second confederate left and the participant remained in the scanner for anatomical image acquisition. At the end of the behavioural replication study, the confederate left and participants remained in the cabin to complete the same questionnaires as in the fMRI study.

Task

Each trial started with a fixation cross displayed for 4000-6000 ms, followed by a continuous slider scale (internally ranging from 0-100) that asked the participant to indicate how close they felt to the other person at this moment ("How close do you feel to the other person?" in German). Participants were asked to respond within 10 seconds (6 seconds in the laboratory study). After a second fixation cross (1000-2000 ms), participants were either shown a fully filled flash in the partner's color (symbolizing a painful stimulation of the partner, i.e., a reinforced trial) or a partly filled flash in the partner's color (symbolizing a non-painful stimulation of the partner, i.e., a non-reinforced trial) for 2000 ms. The respective flash was followed by a fixation cross (1000-2000 ms). At the end of each trial, participants indicated how they felt ("How do you feel?" in German) after having observed the partner's stimulation on a visually displayed continuous slider scale (internally ranging from 0-100), and again had to respond within 10 seconds (6 seconds in the laboratory study). The trial structure is visualized in **Figure 1B**.

Behavioral control study

Procedure

The procedure was identical to the behavioural replication study, except that now the participants were assigned as pain recipients and the confederates could decide to give up money to spare them from pain, a procedure that has been shown to activate the motive to repay this favor (Hein, Morishima, Leiberg, Sul, & Fehr, 2016; Saulin, Horn, Lotze, Kaiser, & Hein, 2022). Similarly to empathy, this social norm of reciprocity can increase closeness (Adams & Miller, 2022; Neyer, Wrzus, Wagner, & Lang, 2011). Inducing reciprocity in the control study allowed us to test if potential learning-related changes in social closeness are specifically related to empathy or generalize to other socially ubiquitous contexts.

Each block of the control learning task consisted of 25 trials. In the treatment condition (corresponding to two interaction blocks with one confederate), participants observed that the partner ostensibly decided to help them in 80% of the trials in block 1 (acquisition phase) and in 20% of the trials in block 2 (extinction). In the control condition (corresponding to the two interaction blocks with the other confederate), participants observed that the partner ostensibly helped them in 50% of the trials in block 1 as well as block 2. Again, the order of the treatment and control condition were counter-balanced across participants. To avoid possible reputation effects (Engelmann & Fischbacher, 2009; Gächter & Falk, 2002), which could influence participants' behavior, at the beginning of the experiment participants were informed that they would not meet the ostensible other participants after the experiment. At the end of the study, the confederate left and participants remained in the cabin to complete the same questionnaires as in the other two studies.

Task

The trial structure was analogous to the fMRI study and the behavioural replication study described above using the same assessment of trial-by-trial social closeness. Each trial started with the display of a jittered fixation cross (4000-6000 ms). Then participants were asked to

indicate how close they felt to the other person at that moment (“How close do you feel to the other person?” in German) on a continuous slider scale (internally ranging from 0-100) and were asked to respond within 6 seconds. After a fixation cross (1000-2000 ms), participants saw a screen, in which the two possible options were visualized side-by-side using a fully filled flash in the color of the participant (symbolizing the option to take the monetary reward and not help the participant) and a crossed out fully filled flash in the color of the participant (symbolizing the option to forego the monetary reward and help). Participants were told that this was the decision screen, which the interaction partner also saw while making her decision to either spare or not spare the participant from painful stimulation. This screen was shown for a jittered length of 2000-4000 ms, followed by the display of the ostensible decision of the interaction partner. If the decision was to help (reinforced trial), the crossed-out flash was highlighted by a box in the color of the interaction partner. If the decision was not to help (non-reinforced trial), the fully filled flash was shown highlighted by a box in the color of the interaction partner. After another fixation cross (1000-2000 ms), the emotion rating scale was shown asking the participant how they felt after observing the partner’s decision (“How do you feel?” in German). Again, participants were asked to respond within 6 seconds. Then, the next trial started.

Table 4. Demographics and average questionnaire score of participants in the three studies. Mean values and standard deviations are reported. N = number of included participants.

	fMRI study	behavioural replication study	behavioural control study
N	46	27	27
age [years]	24.06 (4.52)	22.89 (3.36)	23.07 (3.35)
trait empathic concern	19.07 (3.15)	20 (2.59)	19.45 (3.63)
trait perspective-taking	17.82 (3.14)	18.26 (3.39)	18.07 (3.17)

trait positive reciprocity	5.86 (1.57)	5.89 (1.54)	5.79 (1.59)
impression rating	4.85 (2.05)	4.83 (1.41)	4.83 (1.25)

Questionnaires

At the end of the respective main experiments, participants filled out questionnaires capturing trait empathic concern, and perspective taking/cognitive empathy (empathic concern and perspective taking subscales of the Interpersonal Reactivity Index (IRI, Davis, 1980). Conceptually, scores on the empathic concern subscale have been related to emotional empathy, and scores on the perspective taking subscale to cognitive empathy (Davis, 1980, 1983). Moreover, they completed questionnaires measuring individual differences in trait reciprocity (Perugini, Gallucci, Presaghi, & Ercolani, 2003) as well as participants' impressions of the other individuals (confederates) (Hein, Engelmann, et al., 2016; Hein, Silani, Preuschoff, Batson, & Singer, 2010), modified from (Batson et al., 1988). Questionnaire scores were comparable between studies, all $ps > .29$. Average scores and standard deviations are reported in **Table 4**.

Pain stimulation

In the fMRI study, painful stimulation was applied using a Digitimer DS7A constant current stimulator (Hertfordshire, United Kingdom) and an MRI compatible surface electrode attached to the left lower inner arm. Shock segments consisted of a single 1 ms square-wave pulses. For pain stimulation in the laboratory, we used a mechano-tactile stimulus generated by a small plastic cylinder (612 g). The projectile was shot against the cuticle of the left index finger using air pressure (Impact Stimulator, Labortechnik Franken, Release 1.0.0.34).

Importantly, the intensity of the painful stimulation in all studies was based on the same subjective criterion, determined in an individual pain thresholding procedure. Participants received pain stimulation with slowly increasing intensities starting with the lowest value of 0.00 mA (fMRI study) or 0.25 mg/s (replication and control study) and increasing in steps of 0.05 mA (fMRI study) or 0.25 mg/s (replication and control study), and rated its unpleasantness

on a scale from 1 (no pain at all, but a participant could feel a slight tingling) to 10 (extreme, hardly bearable pain). In the main experiment, a subjective value of 8 (corresponding to a painful, but bearable pain, was used for painful stimulation and a subjective value of 1 was used for non-painful stimulation.

Regression analyses

In all linear mixed effects regression models, we included participant as random intercept in order to account for shared error variance across multiple data points, i.e., the within-subjects variables. Random slopes were included for continuous variables if these variables were also included as a fixed effect. As our categorical variables only yielded two levels, we did not include random slopes for categorical variables.

As a manipulation check, we first checked whether emotion ratings significantly differed for observed pain vs. no-pain. To test this, we ran a linear mixed models analysis with the fixed effects of trial type (reinforced vs. non-reinforced), study (fMRI vs. replication study), and their interaction, participant as random intercept and the dependent variable emotion rating.

In order to test whether we successfully reinforced empathy, we conducted a linear mixed models analysis with empathy subscale (empathic concern and perspective-taking subscales of the IRI, Davis, 2006), trait score, trial type, study, and their interaction as fixed effects, participant and trial number as random intercept, and emotion ratings as dependent variable. In the behavioral control study, the analogous analysis was conducted but using positive reciprocity as trait measure of reciprocity (positive reciprocity) subscale of the PNR (Perugini et al., 2003).

In order to test the influence of condition, block, and trial number on social closeness, we conducted linear mixed models with condition, block (block 1 vs. block 2), trial number (1-25), and study (fMRI vs. replication study) as fixed effects, participant as random intercept, trial number as random intercept for participant and trial-by-trial closeness ratings as dependent variable.

To test whether the neural sensitivity to empathy reinforcers that was related to individual recalibration (see *fMRI statistical analyses* for details) was linked to social closeness in the treatment condition, we conducted two follow-up analyses with neural betas extracted from IFG/AI and STS/TPJ separately, block (acquisition vs. extinction), empathy subscale (empathic concern vs. perspective-taking), and trait score as fixed effects, participant and trial number as random intercept, and social closeness ratings as dependent variable.

Linear mixed model analyses were conducted in R (version 4.0.4) (R Core Team, 2019) using the packages *lme4* (Bates et al., 2014) and *car* (Fox et al., 2018). For mixed models, we report the chi-square values derived from Wald chisquare tests using type 3 sum of squares from the *Anova()* function (*car* package). For predefined contrasts, we report the t-values derived from the *summary()* function. Simple slopes extracted from the linear mixed models are reported with 95% confidence intervals using the *emtrends* function (*emmeans* package (Lenth, Singman, Love, Buerkner, & Herve, 2019)).

Specific Bayesian follow-up mixed models analyses to explicitly test for null effects were conducted using the *brms* package and bayes factors were determined using the function *bayes_factor* (Bürkner, 2021). Bayesian t-tests were conducted using the function *ttestBF* from the package *BayesFactor* (Morey et al., 2022).

Computational modelling

To identify the computational mechanisms of the formation and maintenance of empathy-related social closeness, we tested three different learning models against each other (**Figure 3**). Specifically, our baseline model, which implemented only the standard Rescorla-Wagner learning rule (model 1, **Figure 3A**), was compared to two recent adaptations (models 2 and 3) that allowed us to test the role of specific processes, namely differential learning rates for positive and negative feedback (Garrett & Daw, 2020) and context-dependent recalibration of the prediction error (Bavard, Lebreton, Khamassi, Coricelli, & Palminteri, 2018). The first adaptation assumes different learning rates for positive prediction errors and negative prediction

errors, i.e., for the learning and the unlearning of an association (model 2, **Figure 3B**). If, for example recent experiences more strongly influence surprisingly positive than surprisingly negative feedback, the learning rate for positive prediction errors will be larger than the learning rate for negative prediction errors. In the context of empathy-related and reciprocity-based social closeness such a finding would entail that social closeness more rapidly increases in the acquisition block than it decreases in the extinction block.

In the second adaptation, we hypothesized that the assumed outcome values of the respective feedback (i.e., $R = 1$ for reinforcer feedback and $R = 0$ for non-reinforcer feedback) may vary depending on the respective context (e.g., empathy motive vs. reciprocity motive) (model 3, **Figure 3C**). That is, the outcome value is recalibrated depending on the context. This recomputed outcome value is then used to compute the prediction error which means that the learning signal itself is recalibrated (c.f. Palminteri et al., 2015, p.11 “[...] an outcome should be compared before updating option values.”). The larger this recalibration, the smaller the learning signal associated with a reinforced trial and the larger the learning signal associated with a non-reinforced trial, and vice versa. Context-dependent recalibration therefore allows social closeness to continue to increase in the extinction block despite a high probability for non-reinforced trials.

Based on these models, we aimed to test whether empathy stability can be understood (i) in terms of asymmetrical updating of the learning signal (i.e., different learning rates for reinforced and non-reinforced trials), or (ii) in terms of recalibration of the value associated with the feedback in each trial (i.e., a value different from 1 in reinforced trials and different from 0 in non-reinforced trials). Hence, we tested which out of three models in our model space best describes participants’ behavior.

In the simplest model (*basic model*), the estimated motive-driven closeness V at trial t is updated with prediction error δ and free parameter α only. Specifically, the prediction error is calculated as the difference between the actual outcome and the prediction:

$$\delta_t = R_t - V_{t-1} \tag{1}$$

In equation (1), R refers to the actual outcome: 1 for reinforced feedback (painful stimulation of the partner in the fMRI and behavioral replication study, and decision of the partner to help in the behavioral control study), and 0 for non-reinforced feedback (non-painful stimulation of the partner in studies 1 and 2, and decision of the partner not to help in the control study) at trial t . Afterward, the prediction error from the current trial t will be used to update V at trial t after applying the weighting of the learning rate:

$$V_t = V_{t-1} + a \times \delta_t \quad (2)$$

In the second model (*differential model*), we tested if positive and negative prediction errors are updated separately, inspired by previous studies on reward learning (c.f. Garrett & Daw, 2020). In this model, the prediction error was calculated as in equation (1), but learning rates depended on whether the present trial was reinforced or not (see equation 3). That is, a positive δ will be multiplied by learning rate α^+ , and a negative δ will be multiplied by learning rate α^- to update V .

$$V_t = \begin{cases} V_{t-1} + \alpha^+ \times \delta_t & \text{if } \delta > 0 \\ V_{t-1} + \alpha^- \times \delta_t & \text{if } \delta < 0 \end{cases} \quad (3)$$

Hence, the learning of empathy-related closeness may be characterized by a stronger weight of the prediction error for reinforced compared to non-reinforced trials, thus leading to less decline in empathy-related closeness when reinforcer rates are low (as in the second block of the treatment condition in the fMRI and the behavioral replication studies).

Third, based on previous work (Palminteri et al., 2015), the assumed outcome values of the respective feedback (i.e., $R = 1$ for reinforcer feedback and $R = 0$ for non-reinforcer feedback) may actually be recalibrated depending on the respective context. For the present studies, this context was primarily defined by the respective motive which was reinforced (empathy motive vs. reciprocity motive). Hence, ω may on average be different for individuals in the fMRI study and the behavioral replication study than for individuals in the behavioral control study. To test whether the learning of motive-driven closeness can be understood in these terms, we added a

third model (*individual calibration model*), in which the proposed outcome value is recalibrated by subtracting an additional free parameter ω (see equation 4).

$$\delta_t = |R_t - \omega| - V_{t-1} \quad (4)$$

Hence, according to this model, an individual's actual outcome value for reinforced trials corresponds to 1 minus the individual recalibration value ω , and the actual outcome value of a non-reinforced trial corresponds to ω . Therefore, the larger the value of ω , the more likely a positive prediction error and subsequent increase of social closeness after non-reinforced trials. Moreover, the larger the value of ω , the less the decline of empathy-driven closeness can be expected for the extinction block (i.e., when non-reinforced trials are most frequent).

Exploratory models

Based on the results obtained from the first model comparison and in order to more closely investigate the computational basis of empathy-related social closeness sustainability, we developed a second model space. That is, we tested whether the individual recalibration of the outcome value in these two groups depended on either the condition (treatment vs. control), block (block 1 vs. block 2) or both. The second model space hence comprised four different models either assuming only one general recalibration parameter ω , assuming condition specific recalibration parameters $\omega_{\text{treatment}}$ and ω_{control} , assuming block-specific recalibration parameters $\omega_{\text{block 1}}$ and $\omega_{\text{block 2}}$, or assuming condition- and block-specific recalibration parameters ω_{treat1} , ω_{treat2} , ω_{control1} and ω_{control2} .

We hypothesized that the maintenance of social closeness in the extinction block may be mechanistically subserved by a reversal of the respective feedback value for reinforced and non-reinforced trials (i.e., non-reinforced trials actually become the reinforced trials in block 2 of the treatment condition). Such a reversal should entail a large recalibration of the feedback value in block 2 of the treatment condition, since the larger the recalibration value ω , the more the feedback value of reinforced trials moves closer to 0 (i.e., the original value of non-reinforced trials), and the more the feedback value of non-reinforced trials moves closer to 1

(i.e., the original value of reinforced trials, see **Equation 4**). Hence, it is plausible to assume, that the extent of recalibration may be large in block 2 of the treatment condition, but small in block 1 of the treatment condition. No such differentiation should be observed for the control condition.

In order to test this hypothesis, we tested which out of four new models best described participants' behavior (see **Figure 3-1** for visualization of model space II). Model 1 corresponds to the winning model from model space I (*individual calibration model*), model 2 is an extension of this model in that it assumes different values of recalibration for the treatment and the control condition but across both blocks (*condition-specific recalibration model*), model 3 assumes different values of recalibration for the block 1 and block 2 across both conditions (*block-specific recalibration model*), and model 4 assumes different values of recalibration for block 1 of the treatment condition, block 2 of the treatment condition, block 1 of the control condition, and block 2 of the control condition (*condition and block-specific recalibration model*). If the emotion reversal effect can indeed be understood in terms of outcome value reversal from the first to the second block of the treatment condition, the most complex model (*condition and block specific recalibration model*) should be most likely to have generated the data, revealing moderate recalibration in the two blocks of the control condition, low recalibration in the first block of the treatment condition, and high recalibration in the second block of the treatment condition.

Model optimization and comparison

The parameters θ_M in each model M were optimized using the procedure of minimizing the negative logarithm of the posterior probability (nLPP): the combination of the likelihood for choosing a particular closeness value and the prior distribution of the parameters.

$$nLPP = -\log(P(\theta_M | D, M)) \propto -\log(P(D | M, \theta_M)) - \log(P(\theta_M | M)) \quad (5)$$

$P(D | M, \theta_M)$ refers to the likelihood of choice value D (i.e., the actual rating) given the current model M and its parameters θ_M . Here, we assumed that the rating was selected from

the normal distribution with the estimated rating as mean (given M and θ_M) and standard deviation of 0.4. Therefore, if the rating is correctly estimated and close to the actual rating D , the likelihood will be high. It is worth to note that this method deviates from the typical approach to estimate Q-learning models, in which the probability of a binomial decision is estimated with temperature parameter β . The temperature parameter β explains whether a decision is made based on the differences between two options, however, this is not appropriate in the context of our task that includes only one choice option on a continuous scale.

$P(\theta_M | M)$ is the likelihood of getting an estimate for θ_M within the prior probability distribution of the parameters. All parameters were selected from a beta distribution ($\alpha = \beta = 1.1$) (Daw, Gershman, Seymour, Dayan, & Dolan, 2011), so that the estimated value will always be located between 0 and 1. We then applied the model to fit the data.

A lower LPP value indicates that a model can explain the data better, however, the $nLPP$ does not take a model's complexity into consideration. To address this issue, we then applied the Laplace approximation to the model evidence (*LAME*) to penalize goodness-of-fit (i.e., the measure of $nLPP$ for each subject) with model complexity (i.e., number of parameters). The *LAME* for each model was computed according to equation 6.

$$LAME \equiv -LPP + df/2 \log(2\pi) - 1/2 \log|H| \quad (6)$$

In this calculation, df is determined as the number of free parameters and $|H|$ is the determination of the Hessian. Again, these values were computed at individual level.

To test which model out of the model space is most likely to have generated a certain data set, we fed the *LAME* (from each subject in each model) into group-level random-effects analysis using the *mbb-vb-toolbox* (<http://mbb-team.github.io/VBA-toolbox/>; (Daunizeau, Adam, & Rigoux, 2014)). This toolbox performs Bayesian model selection and estimates two indicators of model performance: the exceedance probability (EP) and the expected model frequencies (EF) for each model. Specifically, the exceedance probability of a model quantifies the probability for a given model to have generated the data relative to the other models in the

model space. Commonly, an EP higher than 95% is an indicator of convincing evidence for a model to be most likely to have generated the data compared to other models. The expected frequency *EF* of a model quantifies the probability that the model generated the data for any randomly selected subject. Note that the EF should be higher than chance level given the number of models in the model space (in our case higher than 1/3).

The modelling was conducted using MATLAB 2018b. The estimated rating (*V*) was initialized as the actual rating in the first trial in each block. All the parameters were optimized using MATLAB's *fmincon* function with random starting points, ranging from 0 to 1.

fMRI data acquisition

Imaging data was collected using a 3T MRI-scanner (Skyra syngo, Siemens, Erlangen, Germany) with a 32-channel head coil. Functional imaging was performed with a multiband EPI sequence of 42 transversal slices oriented along the subjects' anterior to posterior commissure (AC-PC) plane and distance factor of 50% (multi-band acceleration factor of 2). The in plane resolution was $2 \times 2 \text{ mm}^2$ and the slice thickness was 2 mm. The field of view was $216 \times 216 \text{ mm}^2$, corresponding to an acquisition matrix of 108×108 . The repetition time was 1340 ms, the echo time was 25 ms, and the flip angle was 60° . Structural imaging was conducted using a sagittal T1-weighted 3D MPRAGE with 240 slices, and a spatial resolution of $1 \times 1 \times 1 \text{ mm}^3$. The field of view was $256 \times 256 \text{ mm}^2$, corresponding to an acquisition matrix of 256×256 . The repetition time was 2300 ms, the echo time was 2.96 ms, the total acquisition time was 3:50 min, and the flip angle was 9° . We obtained, on average, 1215 (SE = 5.07 volumes) EPI-volumes in the control condition and 1,208 (SE = 4.26 volumes) EPI columns in the treatment condition for each participant. We used a rubber foam head restraint to avoid head movements.

fMRI Preprocessing

Preprocessing and statistical parametric mapping were performed with SPM12 (Wellcome Department of Neuroscience, London, UK) and MATLAB version 9.2 (MathWorks Inc;

Natick, MA). Spatial preprocessing included realignment to the first scan, and unwarping and coregistration to the T1 anatomical volume images. Unwarping of geometrically distorted EPIs was performed using the FieldMap Toolbox. T1-weighted images were segmented to localize grey and white matter, and cerebrospinal fluid. This segmentation was the basis for the creation of a DARTEL Template and spatial normalization to Montreal Neurological Institute (MNI) space, including smoothing with a 6 mm (full width at half maximum) Gaussian Kernel filter to improve the signal-to-noise-ratio. To correct for low-frequency components, a high-pass filter with a cut-off of 128 s was used.

fMRI statistical analysis

First-level analyses

First-level analyses were performed with a general linear model (GLM), using a canonical hemodynamic response function (HRF). Regressor lengths were defined from stimulus onset until the individual response was made by pressing a button (resulting in a time window of 1000 ms + individual response time) for stimuli that required a response (emotion rating phase, closeness rating phase) and from stimulus onset to stimulus offset for stimuli that were just observed by participants (feedback phase, i.e., observing the partner's pain vs. non-pain). The main regressor of interest was the emotion rating phase (scale onset until button press), because this is the phase that is most clearly linked to the explicit empathic reaction. The closeness phase (scale onset until button press) and the feedback phase (stimulus onset until stimulus offset) were added as further regressors to account for variance during these task phases. Parametric modulators coded the trial type (PM trial type), i.e., whether the current trial was reinforced (value = 1) or non-reinforced (value = 0), separately for the closeness phase, the feedback phase, and the emotion rating phase. An additional task of no interest was modelled as additional regressor. The residual effects of head motions were corrected by including the six estimated motion parameters for each participant and each session as regressors of no

interest. To allow for modelling all the conditions in one GLM, an additional regressor of no interest was included, which modelled the potential effects of session.

Second-level analyses

Based on the first-level model, we performed one-sample t-tests on the respective parametric modulator separately for each phase of interest (feedback, emotion-rating, closeness) across all blocks and conditions. In a next step, we computed second-level regressions with the same simple contrasts and individual ω values as covariate across all blocks and conditions for the emotion-rating phase. Next, we re-ran these second-level regressions using the difference in neural activation between conditions, i.e., PM trial type (treatment) > PM trial type (control) and individual ω values as covariate. As recommended, a cluster-forming threshold of $p < .001$ uncorrected (Eklund, Nichols, & Knutsson, 2016; Woo, Krishnan, & Wager, 2014; Yeung, 2018) was used, and where not stated otherwise, whole-brain level family wise error (FWE) cluster-corrected statistics are reported at an α level of $p < .05$.

To test the relationship of neural activation related to individual recalibration with closeness ratings, emotion ratings and trait empathy, beta values during acquisition and extinction in the emotion rating phase were extracted from the resulting bilateral clusters in TPJ/STS and left IFG/AI using MarsBar (Brett, Anton, Valabregue, & Poline, 2002). Extracted beta values were added as predictors in two separate linear mixed models together with block (acquisition vs. extinction) and empathy subscale scores (empathic concern vs. perspective-taking subscale of the IRI, Davis, 2006), trait score, and their interaction as fixed effects, participant and trial number as random intercepts, and social closeness as dependent variable.

Data and Code availability

Data and code are available at github (github.com/AnneSaulin/empathy_social_closeness). The design and the confirmatory analyses were preregistered on the Open Science Framework (<https://osf.io/yz9rq/registrations>).

Results

Results of the fMRI and the behavioural replication study

Manipulation Checks

To confirm that participants differentiated between the two trial types (reinforced vs. non-reinforced), we first tested whether participants' emotional reaction to observed pain differed to observed non-pain. This analysis of the emotion ratings showed a main effect of trial type (pain vs. non-pain) across both studies ($\chi^2 = 524.05$, $p < .001$, $\beta = 1.10$, $SE = .05$), indicating that participants emotionally distinguished between those trials in which the partner received painful stimulation vs. non-painful stimulation in the fMRI study and the replication study. This effect was even stronger in the replication study than in the fMRI study (trial type \times study interaction: $\chi^2 = 32.03$, $p < .001$, $\beta = -.34$, $SE = .06$).

To test whether the emotion ratings were associated with external measures of affective and cognitive empathy, we conducted a linear regression analysis with the emotion ratings as dependent variable, empathic trait (the empathic concern vs. perspective taking subscale of the IRI, Davis, 2006), score (score on the respective subscale), and study (fMRI vs. replication study) as predictors, and trial type (observed pain vs. observed no-pain) as control variables. According to the results, emotion ratings after observing painful stimulation compared to non-painful stimulation were significantly predicted by individual differences in trait scores on the two subscales (main effect of trait score : $\chi^2 = 4.57$, $p = .03$, $\beta = -.27$, $SE = .13$; trait score \times trial type interaction: $\chi^2 = 12.35$, $p < .001$, $\beta = .53$, $SE = .15$) with no significant difference between the two empathy subscales (trait score \times empathy subscale \times trial type interaction: $\chi^2 = .05$, $p = .82$, $\beta = -.04$, $SE = .19$). The results were replicated and even more pronounced in the behavioural replication study (trait score \times trial type \times study interaction: $\chi^2 = 6.91$, $p = .009$, $\beta = -.49$, $SE = .19$). These results suggest that the manipulation successfully reinforced empathy on a trial-by-trial basis.

Empathy-related social closeness resists extinction

The main goal of the current studies was to understand how social closeness based on empathy develops over time in the two blocks and conditions. To this end, a linear mixed model was conducted with trial number (1 to 25), block (block 1 vs block 2), and condition (control vs. treatment) as fixed effects and participant as random intercepts, and trial number as random slope for participant. This analysis revealed that empathy-related closeness increased with trial number in all blocks and conditions (main effect of trial number ($p < .001$, see **Table 1** for full results and **Figure 2A** for visualization). This effect, however, was not modulated by block and condition (trial number \times block \times condition interaction: $p = .103$, $\log(\text{BF}) = -7.41$). Average closeness was larger in block 2 than block 1 (main effect of block: $p < .001$) and larger in the treatment than in the control condition (main effect of condition: $p < .001$). Further, results showed a significant interaction between condition and block ($p < .001$) which was, however, not qualified by differential effects of condition in the two blocks (i.e., all 95% confidence intervals of the simple means based on the model largely overlapped, indicating no significant post-hoc effects). In contrast to a hypothesized decay in social closeness in block 2 of the treatment condition, post-hoc t-tests comparing the means of the last five trials in block 1 and the mean of the last five trials in block 2, revealed no significant difference in closeness ($t(45) = -0.96$, $p = .344$, $\log(\text{BF}) = -1.40$), indicating sustained empathy towards another who is only rarely receiving painful stimulation. The corresponding analysis in the behavioral replication study replicated these results (main effect of condition: $p < .001$, main effect of trial number: $p < .001$; main effect of block: $p < .001$; condition \times block interaction: $p < .001$; trial number \times block \times condition interaction: $p = .400$, $\log(\text{BF}) = -3.47$), with the exception of a larger main effect of block in the behavioral replication study and a more pronounced interaction between condition and block number (block \times study: $\chi^2 = 4.67$, $p = .031$, $\beta = -.07$, $\text{SE} = .03$); block \times condition \times study: $\chi^2 = 7.66$, $p = .006$, $\beta = .13$, $\text{SE} = .05$); **Figures 2A** and **2C**). Again, post-hoc t-tests comparing the means of the last five trials in block 1 and the mean of the last five trials

in block 2, revealed no significant difference in social closeness ($t(26) = 1.29, p = .208, \log(\text{BF}) = -.85$).

These results suggest that participants dynamically changed their social closeness in the acquisition block in which they observed pain stimulation of the other with high frequency, and in the extinction block in which they observed pain stimulation of the other with low frequency. Next, we used computational modelling to clarify the underlying mechanisms.

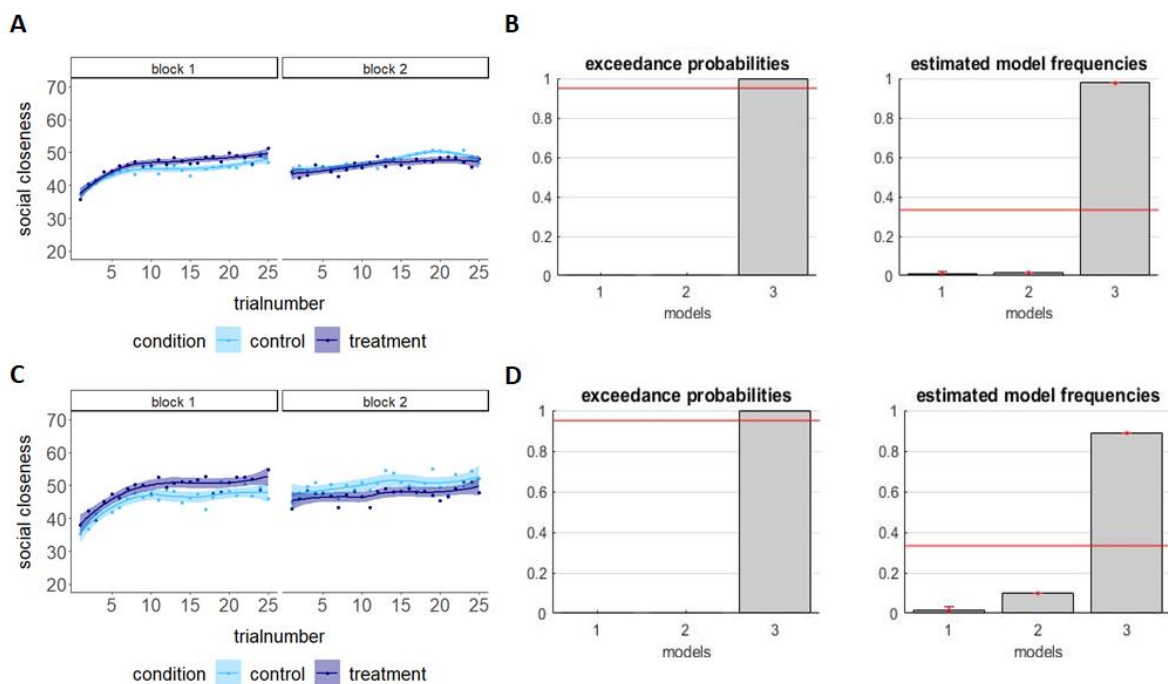


Figure 2. Mean empathy-related social closeness and results of Bayesian model comparison in the fMRI study (top) and the behavioral replication study (bottom). (A) Mean social closeness in the fMRI study with model free trend line and pointwise 95% confidence interval (loess function) by block, condition, and trial number. Social closeness increased in block 1 and plateaus/slightly increased in block 2 in both conditions, demonstrating resistance to extinction of empathy-related social closeness. **(B)** Bayesian model comparison of three models (see **Figure 3** for model space) revealed that individual recalibration of the learning signal associated with observing another’s pain vs. no-pain was most likely to explain participants’ social closeness rating behavior. **(C)** Replication of the behavioral pattern and **(D)** of the modelling comparison results in the behavioral replication study.

Computational modelling of empathy-related social closeness

We tested which of three variants of the Rescorla-Wagner model best described the development of empathy-related social closeness (see **Figure 3** for visualization of the model space and section *Computational Modelling in Materials and Methods* for details). The first model (*basic model*, **Figure 3A**) consisted of the basic Rescorla-Wagner model with one learning rate; the second model (*differential model*, **Figure 3B**) allowed for a different learning rate in reinforced trials and non-reinforced trials; the third model included a recalibration parameter ω that directed the computation of the prediction error (*individual calibration model*, **Figure 3C**).

Bayesian model comparison (see methods for details) revealed that in the fMRI study (**Figure 2B**), the *individual calibration model* is the winning model with an exceedance probability of over 99% (probability that this model is more likely than all other models in the model space) and an estimated model frequency of 97% (probability that this model generated the data of any randomly selected participant). This result was replicated in the behavioral replication study (**Figure 2D**).

Table 1. Effects on empathy-related social closeness. Results of the linear mixed models analysis with condition (treatment vs. control) and trial number (1-25), block (block 1 vs. block 2) as fixed effects, participant as random intercept and trial number as random slope for participant. The dependent variable are participants' closeness ratings in the fMRI study (N = 46, 4600 observations) and the behavioral replication study (N = 27, 2700 observations). χ^2 and $P(\chi^2)$ are the type 3 Wald χ^2 test statistics.

Factor	Beta	SE	t-value	χ^2	P(χ^2)
<i>fMRI study</i>					
(Intercept)	-.076	.129	-.60	.35	.550
Condition	.087	.020	4.30	18.50	<.001
trial number	.096	.024	3.95	15.63	<.001
Block	.140	.020	6.89	47.41	<.001
condition*trial number	.028	.020	1.36	1.85	.174
condition*block	-.149	.030	-5.18	26.87	<.001
trial number*block	-.013	.020	-0.64	.42	.519
condition*trial number*block	-.047	.030	-1.63	2.67	.103
<i>Behavioral replication study</i>					
(Intercept)	-.112	.165	-.68	.46	.496
Condition	.152	.029	5.41	29.27	<.001
trial number	.117	.036	3.28	10.78	.001
Block	.214	.028	7.61	57.98	<.001
condition*trial number	.022	.028	0.78	.62	.431
condition*block	-.283	.040	-7.12	50.68	<.001
trial number*block	-.058	.028	-2.07	4.28	.039
condition*trial number*block	-.035	.040	-.879	.77	.380

The recalibration parameter ω

For empathy-related social closeness, the respective winning model included a recalibration parameter ω . The larger this parameter, the more likely are non-reinforced trials to elicit a positive prediction error and hence a positive updating of closeness. A large ω should thus entail less decay of social closeness in the extinction block than a small ω .

The recalibration parameter ω was initially estimated across all blocks and conditions as one variable characterizing each individual. To test, whether strong recalibration was specific to the extinction block, we assessed four additional models in which ω was free to vary by block, by condition or both. Bayesian model comparison showed that the model allowing for block-specific as well as condition-specific estimations of ω best described participants' behaviour (see **Figure 3-2** for visualization of the Bayesian model comparison results, **Figure 3-5** for comparison metrics, and **Figure 3-4** for visualization of absolute model fit). Analysis of the individual ω showed that on average, participants more strongly recalibrated in the extinction block than in the acquisition block, i.e., on average ω was larger in the extinction block than in the acquisition block (fMRI study: $T(45) = 2.753$, $P = .009$, $CI = [.345, .054]$); replication study ($T(26) = 2.0$, $P = .056$, $CI = [-.005, .384]$), but recalibration values did not significantly differ between block 1 and block 2 for the control condition (fMRI study: $T(45) = -.579$, $P = .568$, $CI = [-.139, .077]$); replication study: $T(26) = -1.027$, $P = .314$, $CI = [-.176, .059]$; for visualization of the median and spread of the extracted parameters, see supplementary **Figure 3-3**). These results indicate that social closeness resisted extinction, because in the extinction block participants updated social closeness based on the observation of no-pain trials, i.e., trials that were defined as non-reinforcers and now elicited positive prediction errors (captured by ω). In contrast, in the acquisition block, participants' changes in empathy-related closeness were driven by observing pain in the other, i.e., the event that was originally defined as the reinforcer.

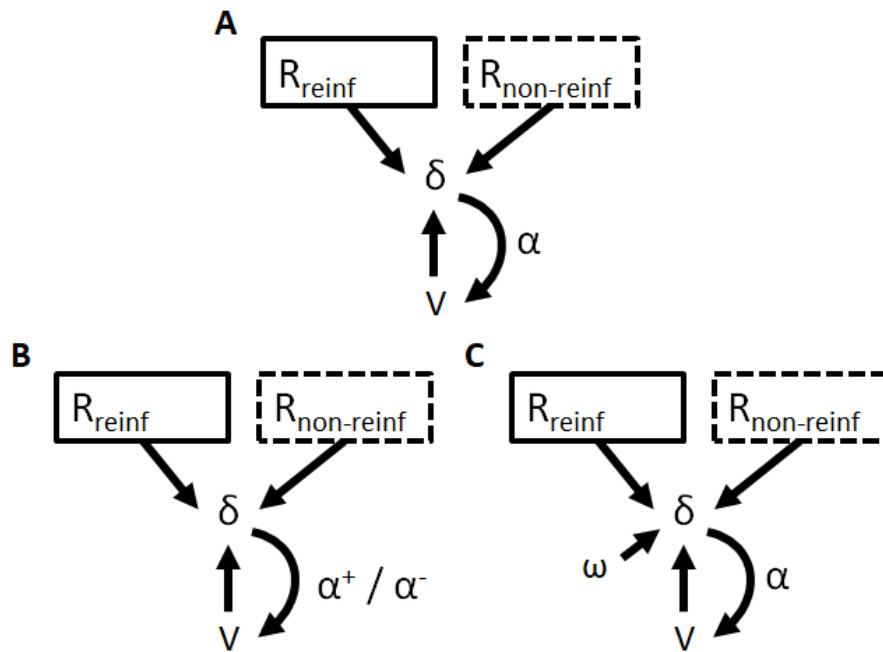


Figure 3. Model space. (A) Basic model. In the basic model, social closeness in the next trial V_t depends on the closeness rating in the present trial V_t and the learning rate α multiplied by the prediction error δ . This prediction error is computed as the difference between the reinforcer value in the current trial R (1 vs. 0) and the closeness rating of the previous trial V_{t-1} . (B) Differential model. Same as the basic model except that alpha is different for reinforced (α^+) and non-reinforced (α^-) trials. (C) Individual calibration model. Same as the basic model except that a recalibration parameter ω is added to the computation of the prediction error δ . That is $\delta = (R - \omega) - V_{t-1}$ if $R = 1$ (reinforced trials = R_{reinf}) and $\delta = \omega - V_{t-1}$ if $R = 0$ (non-reinforced trials = $R_{\text{non-reinf}}$).

Control study

So far, our results revealed that the sustained nature of empathy-related closeness can be understood in terms of the recalibration of the outcome value associated with observing another's pain vs. non-pain. To test if this recalibration of feedback used to update social closeness is a general phenomenon or specifically related to empathy, we conducted a behavioral control study using the identical experimental design to test the formation and

stability of reciprocity-based closeness. Reciprocity, commonly defined as returning a previously given or an anticipated favor (Gouldner, 1960; Hein, Morishima, et al., 2016; McCabe, Rigdon, & Smith, 2003), is one of the most important social norms worldwide (Axelrod & Hamilton, 1981; Falk & Fischbacher, 2006; Nowak, 2006; Perugini et al., 2003). Similar to empathy, reciprocity can increase closeness (Adams & Miller, 2022; Neyer et al., 2011), and is a strong motivator of prosocial behavior (Fehr, Fischbacher, & Gächter, 2002). However, whereas empathy-related closeness and prosociality is elicited by sharing the emotions of the other, reciprocity-based processes are conditional on the other's behaviour, i.e., reflect a "tit-for-tat" principle rather than shared emotions (Dufwenberg & Kirchsteiger, 2004; Eccles, Hughes, Kramár, Wheelwright, & Leibo, 2020; Rand, Ohtsuki, & Nowak, 2009; Zaki, 2014). Hence, to reinforce reciprocity in the present paradigm, the participant received help from the other person, i.e., the other person gave up a monetary reward to save the participant from pain, a procedure that has been-established for enforcing direct positive reciprocity towards the helper (Hein et al., 2010; Saulin et al., 2022). Decisively, the trial structure and the assessment of social closeness was identical to the trial structure in the two empathy studies outlined above.

Manipulation Check

Analogously to the empathy studies above, we first analyzed participants' emotion ratings to test our manipulation. Results of a linear mixed model revealed a main effect of trial type ($\chi^2=62.89$, $p < .001$, $\beta = -1.06$, $SE = .13$) for the reciprocity motive. Thus, participants emotionally distinguished between those trials in which the partner had decided to help them vs. decided not to help them. Moreover, there was a significant relationship between participants' emotion ratings and their scores for positive reciprocity on the trait reciprocity scale (Perugini et al., 2003), ($\chi^2 = 4.34$, $p = .037$, $\beta = .26$, $SE = .12$, confirming that our paradigm successfully reinforced positive reciprocity.

Reciprocity-related social closeness can be extinct

To analyse the development of reciprocity-related social closeness over time, we conducted a linear mixed model with trial number, block, and condition as fixed effects, participant as random intercept and trial number as random slope for participant. This analysis revealed a significant three-way interaction of condition, trial number, and block ($p < .001$), which shows that the development of social closeness over time differentially depended on the block as well as the condition (see **Figure 4A** for visualization and **Table 3** for full results). As such, reciprocity-related social closeness was affected significantly by reinforcement frequency: in the treatment condition (**Figure 4A**, dark lines) social closeness increased when strongly reinforced during the acquisition block (simple slope: $\beta = .02$, 95% Interval = [.01, .03]) and decayed when weakly reinforced during the extinction block ($\beta = -.05$, 95% Interval = [-.06, -.04]), while in the control condition (**Figure 4A**, light lines) where reinforcement remained at chance level in blocks 1 and block 2, little change in social closeness ratings was observed (block 1: $\beta = -.01$, 95% Interval = [-.02, -.004]; block 2: $\beta = -.007$, 95% Interval = [-.02, .001]).

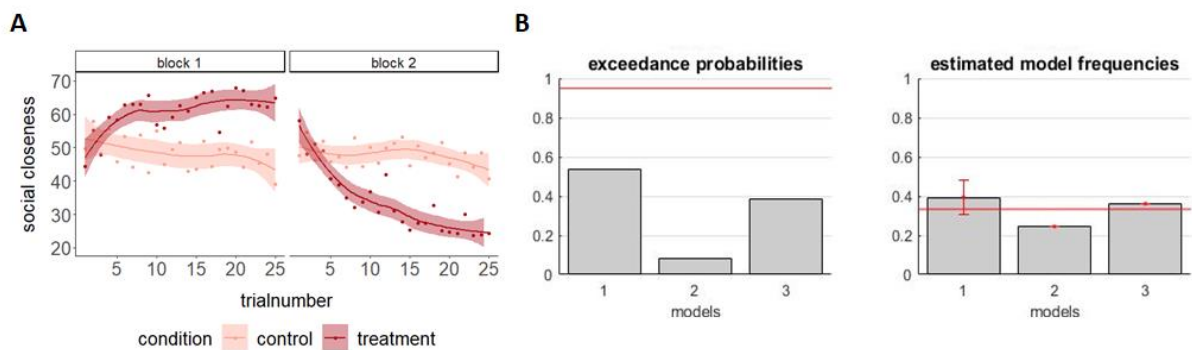


Figure 4. Behavioral pattern and Bayesian model comparison results of the behavioral control study. (A) Mean social closeness with model free trend line and pointwise 95% confidence interval (loess function) by block, condition, and trial number. Social closeness increased in block 1 of the treatment condition (acquisition) and starkly decreased in block 2 (extinction), demonstrating no resistance to extinction of reciprocity-related social closeness. (B) Bayesian model comparison of three models (see **Figure 3** for model space) revealed that the basic model assuming simple updating directly based on the learning signal and individual

recalibration of the learning signal associated with observing another's help vs. no help are equally likely to explain participants' reciprocity-related social closeness rating behavior.

Table 2. Effects on reciprocity-related social closeness. Results of the linear mixed models analysis with condition (treatment vs. control), trial number (1-25), block (block 1 vs. block 2) as fixed effects, participant as random intercept and trial number as random slope for participant. The dependent variable was participants' reciprocity-related closeness ratings in the behavioral control study (N = 27, 2700 observations). χ^2 and $P(\chi^2)$ are the type 3 Wald χ^2 test statistics.

Factor	beta	SE	t-value	χ^2	$P(\chi^2)$
(Intercept)	.034	.126	.27	.07	.789
Condition	.530	.034	15.39	236.85	<.001
trial number	-.082	.028	-2.87	8.25	.004
Block	-.029	.034	-0.83	.70	.403
condition*trial number	.229	.034	6.71	45.07	<.001
condition*block	-1.130	.048	-23.38	546.42	<.001
trial number*block	.030	.034	0.88	0.77	.381
condition*trial number*block	-.530	.048	-11.00	120.70	<.001

Computational modelling of reciprocity-related social closeness

Bayesian model comparison conducted analogously to the fMRI and the behavioral replication study revealed that in the control study, the *basic model* is quite likely to have generated the data as well as the *individual calibration model*. (**Figure 4B**, see **Table 3** for overview of model comparison metrics and **Figure 2-1C** for visualization of absolute model fit). Hence, in contrast to empathy-related social closeness formation and stability, the temporal evolution of reciprocity-related social closeness can also be well captured by a simple learning rule. This is

in line with the decrease in social closeness when the frequency of helping declined in the extinction block, i.e., despite rare helping of the interaction partner.

Table 3. Results of the Bayesian model comparison of the three models in model space I for the three studies. Exceedance probabilities (EP) indicate the likelihood for a given model to have generated the data given the model space. Estimated model frequencies (EF) indicate the likelihood for a model to have generated the data of any randomly selected subject. The absolute value of the laplace approximation to the model evidence (LAME) indicates how well a given model fits the empirical data taking model complexity into account. Lower values indicate better model fit. Where applicable mean values \pm SEs are reported.

Indicator (study)	simple model	differential model	individual recalibration model
<i>fMRI study</i>			
EP	0	0	1
EF	.0075 \pm .00015	.0243 \pm .00049	.9682\pm.00064
LAME	9.1009 \pm .7085	10.6256 \pm .5710	6.7835\pm.4922
<i>Replication study</i>			
EP	0	0	1
EF	.0127 \pm .00043	.0995 \pm .0031	.8879\pm.0034
LAME	9.6402 \pm 1.0080	10.4064 \pm .5754	7.6749\pm.8901
<i>Control study</i>			
EP	.5381	.0783	.3836
EF	.3989\pm.0082	.2451 \pm .0064	.3611 \pm .0080
LAME	9.4270\pm.9857	9.7715 \pm .7127	9.5725 \pm 1.0070

Imaging results

The behavioral results revealed that empathy-related social closeness, in contrast to reciprocity-related social closeness, is robust against extinction, as individuals recalibrate the outcome value associated with observing the other person receive painful vs. non-painful stimulation. Moreover, results from computational modelling indicate that the outcome value of no-pain trials (non-reinforced trials) are associated with positive outcome values and are thus likely to

lead to positive prediction errors, enabling an increase in empathy-related social closeness based on non-reinforced trials.

In a next step, we investigated the neural mechanisms underlying the observed stability of empathy-related closeness. As a manipulation check, we first analyzed the neural activation during participants' emotion ratings after observing painful or non-painful stimulation in the treatment and the control condition as indicator of neural sensitivity to reinforced (painful) as compared to non-reinforced trials (non-painful). A regression analysis with the parametric modulator trial type (painful/ non-painful) revealed an increased activation for the processing of observed painful stimulation in the IFG/ right AI (peak coordinates: $x = 38, y = 28, z = -4$, $p(\text{whole-brain FWE-cluster-corrected}) = .033, k = 143$), the bilateral temporo-parietal junction (TPJ, left hemisphere peak coordinates: $x = -52, y = -52, z = 20, T(44) = 6.21, p < .001, k = 898$; right hemisphere peak coordinates: $x = 62, y = -48, z = 22, T(44) = 4.74, p < .001, k = 532$, see **Figure 5; Figure 5-1**), and the right occipital pole (peak coordinates: $x = 16, y = -92, z = 8, p = .005, k = 214$). Contrasting the results of the parametric regression between the treatment and the control condition revealed no significant results, which is expected given that on average participants observed the same number of pain trials in both conditions.

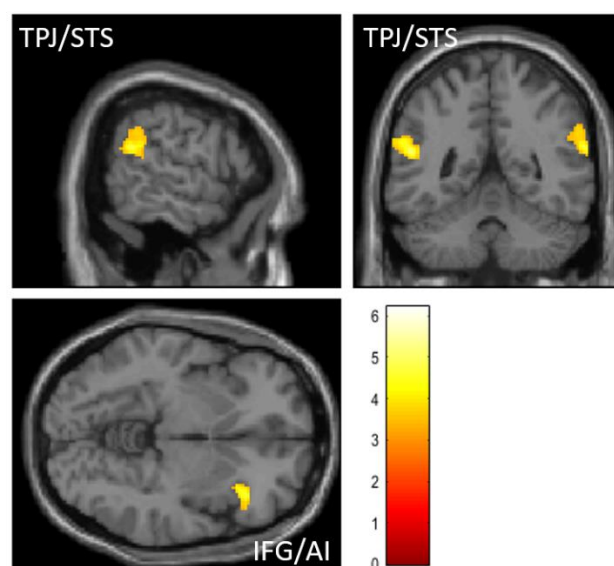


Figure 5. Neural responses to observed pain vs non-pain. Neural activation in the regions for which neural activation was larger in response to observed pain as compared to observed non-pain: bilateral temporo-parietal junction (TPJ) and right inferior frontal gyrus (IFG)/anterior insula (AI). Effects are whole-brain FWE cluster-corrected and visualized at $p < .001$ uncorrected and $k > 50$ voxels.

However, based on the modelling results reported above, the neural effects in the treatment condition in contrast to the control condition, should be modulated by the recalibration parameter, i.e., the parameter that prevented a decline of empathy-related closeness in the extinction block. To test this, first, we exploratorily contrasted the results of the parametric regression with trial type (see analysis above) between the treatment and the control condition, and correlated the individual contrast images with the individual ω -parameter, using a second-level regression. The results revealed significant neural activation in the left IFG extending in to AI (peak coordinates: $x = -32, y = 16, z = 18, t(44) = 4.73, p = .001, k = 269$; **Figure 6A**, upper panel) and the bilateral STS/TPJ (left hemisphere peak coordinates: $x = -66, y = -26, z = 0, t(44) = 5.62, p < .001, k = 517$; right hemisphere peak coordinates: $x = 60, y = -16, z = 10, t(44) = 6.56, p < .001, k = 471$; **Figure 6A**, lower panel; see **Figure 6-1** for full results).

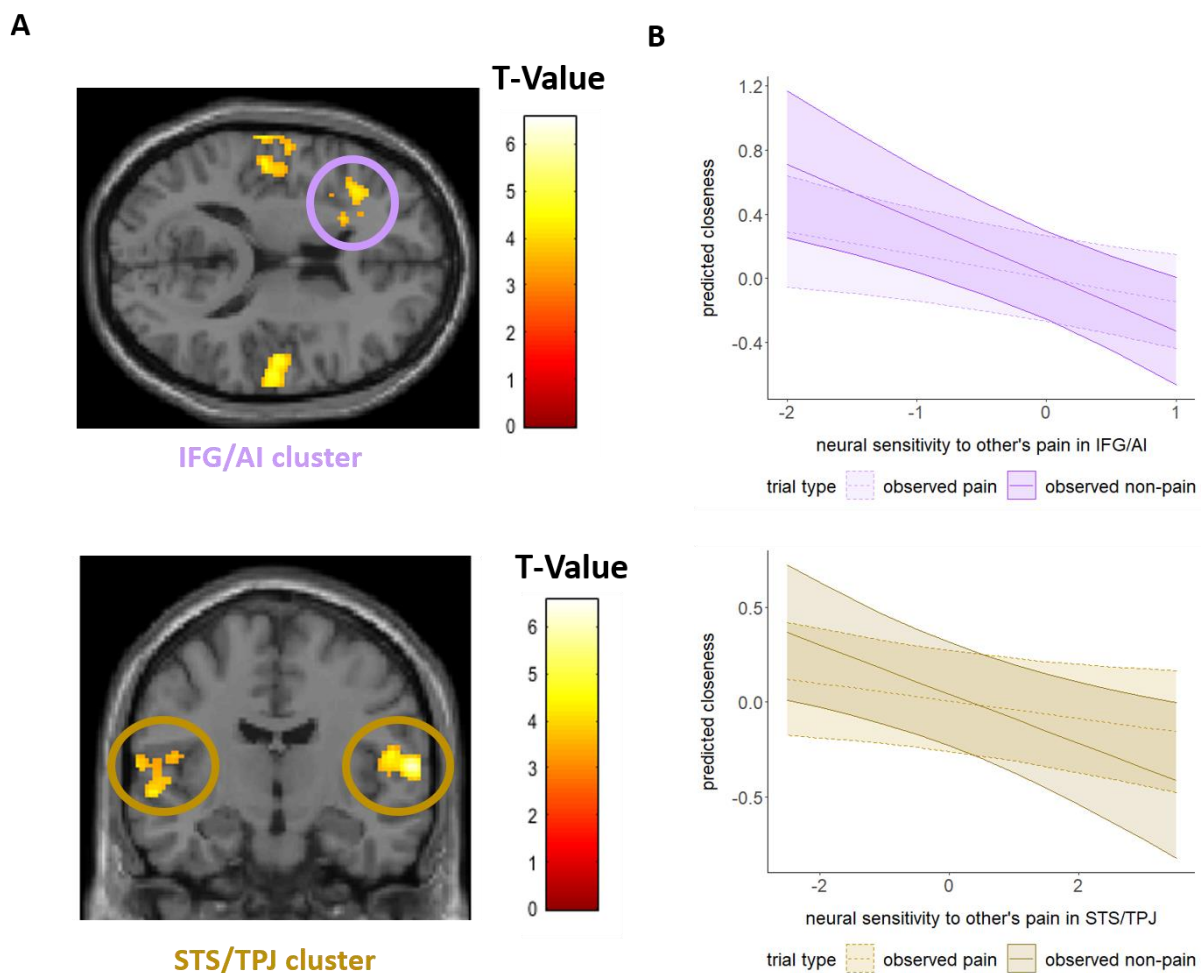


Figure 6. The neural responses to observing painful and non-painful stimulation in others are modulated by the recalibration of the feedback signal (ω) and predict individual changes in social closeness. (A) Regressing the recalibration parameter (ω) against the neural differences in emotion rating-related responses between the treatment and the control condition revealed significant results in the left inferior frontal gyrus and adjacent anterior insula (IFG/AI; upper panel) and the bilateral superior temporal sulcus/ temporal parietal junction (STS/TPJ; lower panel). (B) Relationship between social closeness ratings (averaged over acquisition and extinction as block had no differential effect as expected) and neural sensitivity to trial type in IFG/AI (upper panel) and, STS/TPJ (lower panel). For visualization purposes, maps were thresholded at $p < .001$ uncorrected with cluster size $k \geq 50$. STS = superior temporal sulcus, TPJ = temporo-parietal junction, IFG = inferior frontal gyrus, AI = anterior insula.

In a final step, we tested if the recalibration of the neural sensitivity to the other's pain in IFG/AI and STS/TPJ was indeed related to changes in social closeness depending on whether painful or non-painful stimulation was observed. To do so, we extracted the beta estimates from the entire clusters of IFG/AI and STS/TPJ activation, i.e., from the brain regions for which neural sensitivity to other's pain was related to recalibration (see results of second-level regression above) separately for each block. Next, we conducted two linear mixed models to test whether the recalibration-related neural changes in IFG/AI and STS/TPJ predict social closeness. In a first model, we included the IFG/AI beta estimates, trial type (observed pain vs. observed non-pain), and block (acquisition vs. extinction) as predictors and trial-by-trial social closeness ratings in the respective blocks as dependent variable. Given that trait empathy influenced the emotional reactions on the behavioral level, the two empathy subscales were added as continuous (trait scores) and categorical (scale type: empathic concern vs. perspective-taking) control variables. Results revealed a significant interaction effect of IFG/AI beta estimates and trial type, ($\chi^2 = 5.64$, $p = .018$, $\beta = -.18$, $SE = .07$), reflecting a stronger effect of neural recalibration on social closeness ratings when observing non-pain trials compared to pain trials (**Figure 6B**, upper panel, see **Figure 6-2** for full results). No other effects reached significance (all $ps > .246$).

In a second model, we conducted the analogous analysis with beta estimates from STS/TPJ. The interaction between STS/TPJ and trial type was also significant ($\chi^2 = 6.43$, $p = .011$, $\beta = -.08$, $SE = 0.03$, **Figure 6B**, lower panel, see **Figure 6-3** for full results). There were no other significant effects (all $p > .266$).

Discussion

Here we present the results of two independent studies, showing how empathy-related social closeness is formed and preserved. Using computational modelling, we reveal that empathy-related social closeness is learned if participants repeatedly and frequently observe another

person receiving pain. Importantly, the learned empathy-related social closeness persisted even if the other person is no longer facing frequent pain. This means that social closeness that was generated “in bad times”, i.e., by empathy with the misfortune of another person, is transferred to “good times” in which the other person feels well again.

The computational modelling approach in which we tested different extensions of a standard reinforcement learning model provided insights into the learning mechanisms that allowed for the transition of empathy-related social closeness from “bad times” to “good times”. First, our modelling results revealed that the maintenance of empathy-related social closeness contradicts the assumptions of basic reinforcement learning models. According to these models, empathy-related social closeness should decay if empathy is no longer reinforced. In contrast to this assumption, our data showed that social closeness ratings remained high, even when the participants hardly observed painful stimulation of the other, i.e., the event that had induced empathy-related closeness in the first place. Instead, we found that after they learned empathy-related closeness based on observing pain, participants maintained this social closeness by now learning from positive events (lack of pain) for the other as well. At the computational level, this change in feedback used for learning was captured by a recalibration parameter (ω) which influences the likelihood that formerly non-reinforced trials (here non-pain trials) can elicit a positive prediction error and thus learning. The recalibration of the learning feedback signal linked to the extinction resistance of empathy-related social closeness in our study is in keeping with previous studies that showed that the feedback value is susceptible to different learning contexts and can be individually adjusted (Bavard et al., 2018; Hunter & Daw, 2021; Pischedda, Palminteri, & Coricelli, 2020). The type of context is not decisive as it can take on different forms, such as outcome valence and magnitude (Bavard et al., 2018), uncertainty of reward in a given environment (Hunter & Daw, 2021), or the richness of feedback provided (Pischedda et al., 2020). Extending this previous work, our findings showed that social closeness can be learned from two opposing social feedback signals, i.e., the feedback that another person is in danger (pain) or the feedback that another person is safe (no longer suffering pain). Given

evidence that observing others' pain elicits empathy for pain (Hein, Morishima, et al., 2016; Lamm, Meltzoff, & Decety, 2009; Singer & Klimecki, 2014; Singer et al., 2004) and observing others receiving rewards elicits empathic joy (Andreychik, 2019; Batson et al., 1991), our findings suggest that the *formation* of empathy-related closeness (captured by the processes in the acquisition block) is related to empathy for pain, while the *maintenance* of empathy-related closeness (captured by the processes in the extinction block) is related to empathic joy.

On the neural level, the maintenance of empathy-related closeness was related to activation in bilateral STS/TPJ and left IFG/AI, regions that have been associated with cognitive and affective empathy, respectively. The larger an individual's estimated recalibration parameter was, the more sensitive was the neural activation in these regions in response to another's pain vs. non-pain across all blocks and condition. Follow-up analyses showed that in the treatment condition, the stronger the neural activation in response to another's non-pain vs. pain, the closer participants felt to the other in trials of observed non-pain as compared to trials of observed pain. This suggests that differential neural sensitivity to observed pain and observed non-pain is linked to the stability of empathy-related social closeness.

Underlining the robustness of our results, the finding of sustained empathy-related social closeness and the underlying computational mechanism that we obtained in the fMRI study were replicated in an independent study in the laboratory. Moreover, the specificity of our findings is highlighted by results of a control study. According to the results of the control study, social closeness can also be induced by the social norm of reciprocity. Importantly, however, reciprocity-related social closeness, as opposed to empathy-related social closeness, decays rather quickly despite using the same gradual extinction procedure as for empathy. Specifically, participants showed a learning-related decrease in social closeness if the other person stopped to behave in a reciprocity-evoking manner (reflected by the decrease in closeness ratings in the extinction block). The learning-related changes in reciprocity-based social closeness were well-captured by a basic reinforcement learning model without recalibration for a large portion of the participants. In contrast, the model of empathy-related

closeness required a recalibration parameter to capture the consistently high closeness ratings in the extinction block.

To exclude cross-gender effects, which are likely to occur if female participants interact with male confederates and vice versa, we only tested females. Previous studies have observed that empathic responses on the behavioral and the neural level may differ between men and women (Bluhm, 2017; Christov-Moore et al., 2014). Thus, the present findings may not directly translate to male participants. Future studies are required to show if our results generalize to male participants.

Across the three studies, all experimental parameters were kept constant (e.g., the reinforcer rates in each block) to optimize for comparability. However, for reciprocity, different parameters may be optimal with respect to the formation and stability of social closeness. That said, future studies should test the longevity of reciprocity-related social closeness using a paradigm optimized for reciprocity.

In conclusion and bearing in mind these limitations, the presented results show that empathy-related social closeness, generated in ‘bad times’ transfers to ‘good times’. It has been proposed that empathy is the glue that holds relationships and societies together (Calloway-Thomas et al., 2017; Witenberg & Thome, 2016). The present study provides evidence for the longevity of empathy-related social closeness and reveal the underlying computational and neural mechanisms that may explain why empathy can lead to stable personal and societal relationships.

Acknowledgments

We thank the students who acted as confederates and assisted in data collection.

Funding: This work was supported by the German Research Foundation (GH, HE 4566/6-1; HE 4566/3-2) to GH and by a PhD fellowship by the German Academic Scholarship Foundation

awarded to AS. JBE. gratefully acknowledges support from Amsterdam Brain and Cognition (ABC). CCT was supported by GSSA, MOE Taiwan Scholarship (1081007012).

Author contributions:

Conceptualization: AS, JBE, GH

Methodology: AS, CCT

Software: AS, CCT

Investigation: AS

Formal analysis: AS, CCT

Writing—original draft: AS, GH

Writing—review & editing: AS, CCT, JBE, GH

Visualization: AS

Supervision: JBE, GH

Conflict of interest

The authors declare no competing financial interests.

References

- Adams, M. M., & Miller, J. G. (2022). The flexible nature of everyday reciprocity: reciprocity, helping, and relationship closeness. *Motivation and Emotion*, 1–15.
- Andreychik, M. R. (2019). Feeling your joy helps me to bear feeling your pain: Examining associations between empathy for others' positive versus negative emotions and burnout. *Personality and Individual Differences*, 137, 147–156. <https://doi.org/10.1016/j.paid.2018.08.028>
- Axelrod, R., & Hamilton, W. D. (1981). The Evolution of Cooperation. *Science*. <https://doi.org/10.1126/science.7466396>
- Bates, D., Maechler, M., Bolker, B., Walker, S., Christensen, R. H. B., Singmann, H., ... Eigen, C. (2014). Package "lme4." *Comprehensive R Archive Network (CRAN)*.
- Batson, D., Batson, J. G., Slingsby, J. K., Harrell, K. L., Peekna, H. M., & Todd, R. M. (1991). Empathic Joy and the Empathy-Altruism Hypothesis. *Journal of Personality and Social Psychology*.

<https://doi.org/10.1037/0022-3514.61.3.413>

- Batson, D., Dyck, J. L., Brandt, J. R., Batson, J. G., Powell, A. L., McMaster, M. R., & Griffitt, C. (1988). Five Studies Testing Two New Egoistic Alternatives to the Empathy-Altruism Hypothesis. *Journal of Personality and Social Psychology*, *55*(1), 52–77. <https://doi.org/10.1037/0022-3514.55.1.52>
- Baumeister, R. F., & Leary, M. R. (2017). The need to belong: Desire for interpersonal attachments as a fundamental human motivation. *Interpersonal Development*, *57*–89.
- Bavard, S., Lebreton, M., Khamassi, M., Coricelli, G., & Palminteri, S. (2018). Reference-point centering and range-adaptation enhance human reinforcement learning at the cost of irrational preferences. *Nature Communications*, *9*(1). <https://doi.org/10.1038/s41467-018-06781-2>
- Beeney, J. E., Franklin, R. G., Levy, K. N., & Adams, R. B. (2011). I feel your pain: emotional closeness modulates neural responses to empathically experienced rejection. *Social Neuroscience*, *6*(4), 369–376. <https://doi.org/10.1080/17470919.2011.557245>
- Bluhm, R. (2017). Gender and empathy. In *The Routledge handbook of philosophy of empathy* (pp. 377–387). Routledge.
- Brett, M., Anton, J., Valabregue, R., & Poline, J. (2002). Region of interest analysis using the MarsBar toolbox for SPM 99. *Neuroimage*.
- Brown, S. L., Fredrickson, B. L., Wirth, M. M., Poulin, M. J., Meier, E. A., Heaphy, E. D., ... Schultheiss, O. C. (2009). Social closeness increases salivary progesterone in humans. *Hormones and Behavior*, *56*(1), 108–111. <https://doi.org/10.1016/j.yhbeh.2009.03.022>
- Bürkner, P.-C. (2021). Bayesian Item Response Modeling in {R} with {brms} and {Stan}. *Journal of Statistical Software*, *100*(5), 1–54. <https://doi.org/10.18637/jss.v100.i05>
- Calloway-Thomas, C., Arasaratnam-Smith, L. A., & Deardorff, D. K. (2017). The role of empathy in fostering intercultural competence. In *Intercultural competence in higher education* (pp. 32–42). Routledge.
- Christov-Moore, L., Simpson, E. A., Coudé, G., Grigaityte, K., Iacoboni, M., & Ferrari, P. F. (2014). Empathy: Gender effects in brain and behavior. *Neuroscience and Biobehavioral Reviews*, *46*(4), 604–627. <https://doi.org/10.1016/j.neubiorev.2014.09.001>
- Cowan, T., Pham, A. T., Elvevåg, B., & Cohen, A. S. (2021). Social closeness and cognitive functioning increase feelings of hope for individuals in inpatient treatment. *Psychiatry Research Communications*, *1*(2), 100011. <https://doi.org/https://doi.org/10.1016/j.psycom.2021.100011>
- Cutler, J., & Campbell-Meiklejohn, D. (2019). A comparative fMRI meta-analysis of altruistic and strategic decisions to give. *NeuroImage*, *184*, 227–241. <https://doi.org/10.1016/j.neuroimage.2018.09.009>
- Daunizeau, J., Adam, V., & Rigoux, L. (2014). VBA: A Probabilistic Treatment of Nonlinear Models for

- Neurobiological and Behavioural Data. *PLoS Computational Biology*.
<https://doi.org/10.1371/journal.pcbi.1003441>
- Davis, M. H. (1980). A multidimensional approach to individual differences in empathy. *JSAS Catalog of Selected Documents in Psychology*. <https://doi.org/10.1.1.462.7754>
- Davis, M. H. (1983). Measuring individual differences in empathy: Evidence for a multidimensional approach. *Journal of Personality and Social Psychology*, *44*(1), 113.
- Davis, M. H. (2006). Empathy. In *Handbook of the sociology of emotions* (pp. 443–466). Springer.
- Daw, N. D., Gershman, S. J., Seymour, B., Dayan, P., & Dolan, R. J. (2011). Model-based influences on humans' choices and striatal prediction errors. *Neuron*. <https://doi.org/10.1016/j.neuron.2011.02.027>
- de Waal, F. B. M., Leimgruber, K., & Greenberg, A. R. (2008). Giving is self-rewarding for monkeys. *Proceedings of the National Academy of Sciences*. <https://doi.org/10.1073/pnas.0807060105>
- Dempsey, C. L., Benedek, D. M., Nock, M. K., Zuromski, K. L., Brent, D. A., Ao, J., ... others. (2021). Social closeness and support are associated with lower risk of suicide among US Army soldiers. *Suicide and Life-Threatening Behavior*, *51*(5), 940–954.
- Dufwenberg, M., & Kirchsteiger, G. (2004). A theory of sequential reciprocity. *Games and Economic Behavior*, *47*(2), 268–298.
- Dunsmoor, J. E., Kroes, M. C. W., Moscatelli, C. M., Evans, M. D., Davachi, L., & Phelps, E. A. (2018). Event segmentation protects emotional memories from competing experiences encoded close in time. *Nature Human Behaviour*, *2*(4), 291–299. <https://doi.org/10.1038/s41562-018-0317-4>
- Dvash, J., & Shamay-Tsoory, S. G. (2014). Theory of mind and empathy as multidimensional constructs: Neurological foundations. *Topics in Language Disorders*, *34*(4), 282–295.
<https://doi.org/10.1097/TLD.0000000000000040>
- Eccles, T., Hughes, E., Kramár, J., Wheelwright, S., & Leibo, J. Z. (2020). Learning reciprocity in complex sequential social dilemmas. *Trends in Cognitive Sciences*, *24*(10), 802–813.
- Eklund, A., Nichols, T. E., & Knutsson, H. (2016). Cluster failure: Why fMRI inferences for spatial extent have inflated false-positive rates. *Proceedings of the National Academy of Sciences of the United States of America*, *113*(28), 7900–7905. <https://doi.org/10.1073/pnas.1602413113>
- Engelmann, D., & Fischbacher, U. (2009). Indirect reciprocity and strategic reputation building in an experimental helping game. *Games and Economic Behavior*. <https://doi.org/10.1016/j.geb.2008.12.006>
- Falk, A., & Fischbacher, U. (2006). A theory of reciprocity. *Games and Economic Behavior*.
<https://doi.org/10.1016/j.geb.2005.03.001>
- Fan, Y., Duncan, N. W., de Greck, M., & Northoff, G. (2011). Is there a core neural network in empathy? An

- fMRI based quantitative meta-analysis. *Neuroscience and Biobehavioral Reviews*, 35(3), 903–911.
<https://doi.org/10.1016/j.neubiorev.2010.10.009>
- Fehr, E., Fischbacher, U., & Gächter, S. (2002). Strong reciprocity, human cooperation, and the enforcement of social norms. *Human Nature*. <https://doi.org/10.1007/s12110-002-1012-7>
- Fox, J., Weisberg, S., Price, B., Adler, D., Bates, D., & Baud-Bovy, G. (2018). Package “car.” *R Documentation*.
- Gächter, S., & Falk, A. (2002). Reputation and reciprocity: Consequences for the labour relation. *Scandinavian Journal of Economics*. <https://doi.org/10.1111/1467-9442.00269>
- Garrett, N., & Daw, N. D. (2020). Biased belief updating and suboptimal choice in foraging decisions. *Nature Communications*, 11(1). <https://doi.org/10.1038/s41467-020-16964-5>
- Gouldner, A. W. (1960). The Norm of Reciprocity: A Preliminary Statement. *American Sociological Review*, 25(2), 161–178.
- Grynberg, D., & Konrath, S. (2020). The closer you feel, the more you care: Positive associations between closeness, pain intensity rating, empathic concern and personal distress to someone in pain. *Acta Psychologica*, 210, 1031–1075. <https://doi.org/10.1016/J.ACTPSY.2020.103175>
- Hein, G., Engelmann, J. B., Vollberg, M. C., & Tobler, P. N. (2016). How learning shapes the empathic brain. *Proceedings of the National Academy of Sciences*, 113(1), 80–85.
<https://doi.org/10.1073/pnas.1514539112>
- Hein, G., Morishima, Y., Leiberg, S., Sul, S., & Fehr, E. (2016). The brain’s functional network architecture reveals human motives. *Science*, 351(6277), 1074–1078. <https://doi.org/DOI:10.1126/science.aac7992>
- Hein, G., Qi, Y., & Han, S. (2021). The biological foundations and modulation of empathy. In P. A. M. Van Lange, E. T. Higgins, & A. W. Kruglanski (Eds.), *Social Psychology: Handbook of Basic Principles (Third Edition)* (pp. 127–140). New York: The Guilford Press.
- Hein, G., Silani, G., Preuschoff, K., Batson, D., & Singer, T. (2010). Neural responses to ingroup and outgroup members’ suffering predict individual differences in costly helping. *Neuron*, 68(1), 149–160.
<https://doi.org/10.1016/j.neuron.2010.09.003>
- Hill, C. A. (2009). Affiliation motivation. In M. R. Leary & R. H. Hoyle (Eds.), *Handbook of individual differences in social behavior* (pp. 410–425). New York: The Guilford Press.
- Hunter, L. E., & Daw, N. D. (2021). Context-sensitive valuation and learning. *Current Opinion in Behavioral Sciences*. <https://doi.org/10.1016/j.cobeha.2021.05.001>
- Kok, B. E., & Fredrickson, B. L. (2014). Wellbeing Begins with “We” The Physical and Mental Health Benefits of Interventions that Increase Social Closeness. *Wellbeing: A Complete Reference Guide*, 1–29.
- Krienen, F. M., Tu, P.-C., & Buckner, R. L. (2010). Clan mentality: evidence that the medial prefrontal cortex

- responds to close others. *Journal of Neuroscience*, 30(41), 13906–13915.
- Lamm, C., Batson, D., & Decety, J. (2007). The neural substrate of human empathy: Effects of perspective-taking and cognitive appraisal. *Journal of Cognitive Neuroscience*.
<https://doi.org/10.1162/jocn.2007.19.1.42>
- Lamm, C., Meltzoff, A. N., & Decety, J. (2009). How Do We Empathize with Someone Who Is Not Like Us? A Functional Magnetic Resonance Imaging Study. *Journal of Cognitive Neuroscience*, 22(2), 362–376.
<https://doi.org/10.1162/jocn.2009.21186>
- Lenth, R., Singman, H., Love, J., Buerkner, P., & Herve, M. (2019). Emmeans package: Estimated Marginal means, aka Least-Squares Means. *R Package Version 1.15-15*.
- Lockwood, P. L., Apps, M. A. J., Valton, V., Viding, E., & Roiser, J. P. (2016). Neurocomputational mechanisms of prosocial learning and links to empathy. *Proceedings of the National Academy of Sciences*, 113(35), 9763–9768. <https://doi.org/10.1073/pnas.1603198113>
- Marsh, A. A. (2018). The neuroscience of empathy. *Current Opinion in Behavioral Sciences*, 19, 110–115.
<https://doi.org/10.1016/j.cobeha.2017.12.016>
- McCabe, K. A., Rigdon, M. L., & Smith, V. L. (2003). Positive reciprocity and intentions in trust games. *Journal of Economic Behavior and Organization*, 52(2), 267–275. [https://doi.org/10.1016/S0167-2681\(03\)00003-9](https://doi.org/10.1016/S0167-2681(03)00003-9)
- Morelli, S. A., Lieberman, M. D., & Zaki, J. (2015). The emerging study of positive empathy. *Social and Personality Psychology Compass*, 9(2), 57–68. <https://doi.org/10.1111/spc3.12157>
- Morey, R. D., Rouder, J. N., Jamil, T., Urbanek, S., Forner, K., & Ly, A. (2022). BayesFactor.
- Müller-Pinzler, L., Rademacher, L., Paulus, F. M., & Krach, S. (2015). When your friends make you cringe: social closeness modulates vicarious embarrassment-related neural activity. *Social Cognitive and Affective Neuroscience*, 1–10. <https://doi.org/10.1093/scan/nsv130>
- Neyer, F. J., Wrzus, C., Wagner, J., & Lang, F. R. (2011). Principles of relationship differentiation. *European Psychologist*. <https://doi.org/10.1027/1016-9040/a000055>
- Nowak, M. A. (2006). Five Rules for the Evolution of Cooperation. *Science*, 314(5805), 1560–1563.
<https://doi.org/10.1126/science.1133755>
- Palminteri, S., Khamassi, M., Joffily, M., & Coricelli, G. (2015). Contextual modulation of value signals in reward and punishment learning. *Nature Communications*, 6. <https://doi.org/10.1038/ncomms9096>
- Passarelli, T. O., & Buchanan, T. W. (2020). How Do Stress and Social Closeness Impact Prosocial Behavior? *Experimental Psychology*. <https://doi.org/10.1027/1618-3169/a000482>
- Perugini, M., Gallucci, M., Presaghi, F., & Ercolani, A. P. (2003). The Personal Norm of Reciprocity. *European Journal of Personality*. <https://doi.org/10.1002/per.474>

- Pischedda, D., Palminteri, S., & Coricelli, G. (2020). The effect of counterfactual information on outcome value coding in medial prefrontal and cingulate cortex: From an absolute to a relative neural code. *The Journal of Neuroscience*. <https://doi.org/10.1101/2020.01.08.898841>
- Preckel, K., Kanske, P., & Singer, T. (2018). On the interaction of social affect and cognition: empathy, compassion and theory of mind. *Current Opinion in Behavioral Sciences*, *19*, 1–6. <https://doi.org/10.1016/j.cobeha.2017.07.010>
- R Core Team. (2019). R: A Language and Environment for Statistical Computing.
- Rand, D. G., Ohtsuki, H., & Nowak, M. A. (2009). Direct reciprocity with costly punishment: Generous tit-for-tat prevails. *Journal of Theoretical Biology*. <https://doi.org/10.1016/j.jtbi.2008.09.015>
- Rescorla, R. A., & Wagner, A. R. (1972). A Theory of Pavlovian Conditioning: Variations in the Effectiveness of Reinforcement and Nonreinforcement. In A. H. Black & W.F. Prokasy (Eds.), *Classical conditioning II: current research and theory* (pp. 64–99). New York: Appleton Century Crofts.
- Saulin, A., Horn, U., Lotze, M., Kaiser, J., & Hein, G. (2022). The neural computation of human prosocial choices in complex motivational states. *NeuroImage*, *247*, 118827. <https://doi.org/10.1016/J.NEUROIMAGE.2021.118827>
- Schurz, M., Radua, J., Tholen, M. G., Maliske, L., Margulies, D. S., Mars, R. B., ... Kanske, P. (2021). Toward a hierarchical model of social cognition: A neuroimaging meta-analysis and integrative review of empathy and theory of mind. *Psychological Bulletin*, *147*(3), 293–327. <https://doi.org/10.1037/bul0000303>
- Shiban, Y., Wittmann, J., Weißinger, M., & Mühlberger, A. (2015). Gradual extinction reduces reinstatement. *Frontiers in Behavioral Neuroscience*, *9*. <https://doi.org/10.3389/fnbeh.2015.00254>
- Singer, T., & Klimecki, O. M. (2014). Empathy and compassion. *Current Biology*. <https://doi.org/10.1016/j.cub.2014.06.054>
- Singer, T., Seymour, B., O’Doherty, J., Kaube, H., Dolan, R. J., & Frith, C. D. (2004). Empathy for Pain Involves the Affective but not Sensory Components of Pain. *Science*. <https://doi.org/10.1126/science.1093535>
- Spaans, J. P., Burke, S. M., Altikulaç, S., Braams, B. R., Op De Macks, Z. A., & Crone, E. A. (2018). Win for your kin: Neural responses to personal and vicarious rewards when mothers win for their adolescent children. *PLoS ONE*. <https://doi.org/10.1371/journal.pone.0198663>
- Stevens, F., & Taber, K. (2021). The neuroscience of empathy and compassion in pro-social behavior. *Neuropsychologia*, *159*, 107925.
- Stietz, J., Jauk, E., Krach, S., & Kanske, P. (2019). Dissociating empathy from perspective-taking: Evidence from intra- And inter-individual differences research. *Frontiers in Psychiatry*, *10*, 126.

<https://doi.org/10.3389/fpsy.2019.00126>

Walter, H. (2012). Social Cognitive Neuroscience of Empathy: Concepts, Circuits, and Genes. *Emotion Review*, 4(1), 9–17. <https://doi.org/10.1177/1754073911421379>

Weisz, E., & Zaki, J. (2018). Motivated empathy: a social neuroscience perspective. *Current Opinion in Psychology*, 24, 67–71.

Witenberg, R. T., & Thomae, M. (2016). *Tolerance: the Glue that Binds Us: Empathy Fairness and Reason*. Nova Publishers.

Woo, C.-W., Krishnan, A., & Wager, T. D. (2014). Cluster-extent based thresholding in fMRI analyses: Pitfalls and recommendations. *NeuroImage*, 91, 412–419. <https://doi.org/10.1016/j.neuroimage.2013.12.058>

Xu, X., Zuo, X., Wang, X., & Han, S. (2009). Do You Feel My Pain? Racial Group Membership Modulates Empathic Neural Responses. *Journal of Neuroscience*. <https://doi.org/10.1523/JNEUROSCI.2418-09.2009>

Yeung, A. W. K. (2018). An updated survey on statistical thresholding and sample size of fMRI studies. *Frontiers in Human Neuroscience*, 12(1), 1–7. <https://doi.org/10.3389/fnhum.2018.00016>

Zaki, J. (2014). Empathy: a motivated account. *Psychological Bulletin*, 140(6), 1608–1647. <https://doi.org/10.1037/A0037679>